Longitudinal Study of Cone Photoreceptors during Retinal Degeneration and in Response to Ciliary Neurotrophic Factor Treatment

Katherine E. Talcott,[1] *Kavitha Ratnam,*[1] *Sanna M. Sundquist,*[1] *Anna S. Lucero,*[1] *Brandon J. Lujan,*[2] *Weng Tao,*[3] *Travis C. Porco,*[4] *Austin Roorda,*[2] *and Jacque L. Duncan*[1]

Purpose. To study cone photoreceptor structure and function in patients with inherited retinal degenerations treated with sustained-release ciliary neurotrophic factor (CNTF).

Methods. Two patients with retinitis pigmentosa and one with Usher syndrome type 2 who participated in a phase 2 clinical trial received CNTF delivered by an encapsulated cell technology implant in one eye and sham surgery in the contralateral eye. Patients were followed longitudinally over 30 to 35 months. Adaptive optics scanning laser ophthalmoscopy (AOSLO) provided high-resolution images at baseline and at 3, 6, 12, 18, and 24 months. AOSLO measures of cone spacing and density and optical coherence tomography measures of retinal thickness were correlated with visual function, including visual acuity (VA), visual field sensitivity, and full-field electroretinography (ERG).

Results. No significant changes in VA, visual field sensitivity, or ERG responses were observed in either eye of the three patients over 24 months. Outer retinal layers were significantly thicker in CNTF-treated eyes than in sham-treated eyes ($P < 0.005$). Cone spacing increased by 2.9% more per year in sham-treated eyes than in CNTF-treated eyes ($P < 0.001$, linear mixed model), and cone density decreased by 9.1%, or 223 cones/degree^2 more per year in sham-treated than in CNTF-treated eyes ($P = 0.002$, linear mixed model).

Conclusions. AOSLO images provided a sensitive measure of disease progression and treatment response in patients with inherited retinal degenerations. Larger studies of cone structure using high-resolution imaging techniques are urgently needed to evaluate the effect of CNTF treatment in patients with inherited retinal degenerations. (ClinicalTrials.gov number, NCT00447980.) (*Invest Ophthalmol Vis Sci.* 2011;52: 2219–2226) DOI:10.1167/iovs.10-6479

Inherited retinal degenerations represent a genetically heterogeneous group of diseases that include retinitis pigmentosa (RP) and Usher syndrome type 2. Retinal degenerations are characterized by slowly progressive death of rod and cone photoreceptors and relentless vision loss.[1] One of the challenges that has hampered the development of treatments that may slow vision loss in retinal degeneration is the lack of sensitive outcome measures of disease progression.[2] Objective, sensitive measures of photoreceptor survival may reduce the time required to identify a treatment effect of an experimental therapy.

Neurotrophic factors such as ciliary neurotrophic factor (CNTF) have shown promise in slowing the progression of retinal degeneration.[3,4] Recent studies suggest CNTF can prevent and reverse secondary cone degeneration caused by a mutation in rhodopsin, a rod-specific gene.[5] A phase 1 study[6] of CNTF delivered by intravitreal implantation of a device containing encapsulated cells transfected with the human *CNTF* gene showed promising results in 10 patients with inherited retinal degeneration. Two phase 2 studies were initiated in patients with earlier (CNTF4; ClinicalTrials.gov number, NCT00447980) and later stage (CNTF3; ClinicalTrials.gov number, NCT00447993) inherited retinal degeneration. The objective of the CNTF4 study was to investigate whether CNTF treatment slows the loss of visual field sensitivity relative to the contralateral control eye over 24 months. However, natural history studies of retinal degeneration predict that significant changes in visual function may be measured reliably only after more than 7 years,[7–9] suggesting that significant photoreceptor loss is necessary before changes in visual acuity function can be measured reliably. Outcome measures with greater sensitivity than standard measures of visual function can provide are urgently needed to assess photoreceptors during disease progression and in response to experimental treatments such as CNTF in eyes with retinal degeneration.

Standard clinical imaging techniques cannot visualize individual photoreceptors because of optical imperfections in living eyes. However, adaptive optics (AO) ophthalmoscopy, including adaptive optics scanning laser ophthalmoscopy (AOSLO), can produce images of individual cone photoreceptors noninvasively in living eyes.[10–12] Direct visualization of cones allows comparison of cone spacing and density and, in

From the [1]Department of Ophthalmology, and [4]Francis I. Proctor Foundation for Research in Ophthalmology, Department of Epidemiology and Biostatistics, Division of Preventive Medicine and Public Health, Department of Ophthalmology, University of California at San Francisco, San Francisco, California; [2]School of Optometry, University of California at Berkeley, Berkeley, California; and [3]Neurotech USA, Lincoln, Rhode Island.

Supported by a Career Development Award, Physician Scientist Award and Unrestricted Grant from the Research to Prevent Blindness (JLD); a Career Development Award and a Clinical Center Grant from the Foundation Fighting Blindness (JLD, AR); National Institutes of Health/National Eye Institute Grants EY002162 (JLD) and EY014375 (AR), NIH/NCRR/OD UCSF-CTSI Grant TL1 RR024129 (KET), and K12 EY017269 (BJL); That Man May See, Inc. (JLD, TCP); The Bernard A. Newcomb Macular Degeneration Fund (JLD); Hope for Vision (JLD); the Karl Kirchgessner Foundation (JLD); and NSF Science and Technology Center for Adaptive Optics, managed by the University of California at Santa Cruz under cooperative agreement AST-9876783 (AR).

Submitted for publication August 26, 2010; revised October 13, 2010; accepted October 25, 2010.

Disclosure: **K.E. Talcott**, None; **K. Ratnam**, None; **S.M. Sundquist**, None; **A.S. Lucero**, None; **B.J. Lujan**, Carl Zeiss Meditec, Inc. (C); **W. Tao**, Neurotech USA, Inc. (E); **T.C. Porco**, None; **A. Roorda**, P; **J.L. Duncan**, None

Corresponding author: Jacque L. Duncan, Beckman Vision Center, School of Medicine, University of California at San Francisco, 10 Koret Way, Room K-129, San Francisco, CA 94143-0730; duncanj@vision.ucsf.edu.

ideal situations, tracking of individual cones longitudinally. Cone spacing and density have been used to characterize both normal eyes and eyes with retinal degeneration.[11,13–20] However, they have not been used to track disease progression or response to treatment, including CNTF, in eyes with retinal degeneration.

We present the first images of individual cone photoreceptors observed longitudinally in normal eyes and in patients with inherited retinal degenerations during disease progression. We also report changes in cone photoreceptor structure in response to CNTF therapy in three patients with inherited retinal degenerations participating in the CNTF4 phase 2 clinical trial.

Materials and Methods

This prospective study of 3 of the 68 participants enrolled in the CNTF4 phase 2 study was conducted at a single center where AOSLO images were acquired. Research procedures followed the tenets of the Declaration of Helsinki. Informed consent was obtained from all subjects after explanation of the nature and possible consequences of the studies. The study protocol was approved by the institutional review boards of the University of California, San Francisco and the University of California, Berkeley.

Clinical Examination

Patients were enrolled between April 13, 2007, and May 18, 2007. On the day of surgery, one eye was randomly assigned to receive sustained-release CNTF (NT-501; Neurotech, Lincoln, RI) while the contralateral eye received sham surgery. Additionally, patients were randomly assigned to receive a higher- or lower-dose implant and were masked to both randomizations. The CNTF delivery rate of the implant was determined before implantation by ELISA (R&D Systems, Minneapolis, MN), with the low-dose implant secreting 5 ng/d and the high-dose implant secreting 20 ng/d CNTF. Patients were evaluated at three baseline visits, then at 3, 6, 12, 18, 24, and 30 months after surgery with best-corrected visual acuity, Early Treatment of Diabetic Retinopathy Study (ETDRS) score, and visual field sensitivity measured with automated perimetry using a Humphrey visual field 30–2 test repeated four times at each visit (HFA II 750-6116-12.6; Carl Zeiss Meditec, Inc., Dublin, CA). Time-domain OCT (Stratus OCT 4.0.2 software; Zeiss Instruments, Dublin, CA) images were obtained at baseline and at 12, 24, and 30 months; central foveal thickness from the fast macular thickness map and macular volume were analyzed. Spectral-domain OCT images (Spectralis HRA + OCT Laser Scanning Camera System, Heidelberg Engineering, Vista, CA) were obtained at study visits beginning 12 months after surgery. Twenty-degree horizontal OCT scans were acquired through the anatomic fovea; central foveal thickness and volume were measured.[21] Full-field electroretinogram (ERG) responses were measured according to International Society for Clinical Electrophysiology of Vision standards as previously described.[20] Genetic testing was performed in patient 1 at The John and Marcia Carver Nonprofit Genetic Testing Laboratory (Iowa City, IA). Patients were given the option to have the implant (NT-501; Neurotech) removed after 24 to 30 months.

AOSLO Image Acquisition and Cone Analysis

High-resolution images of cone photoreceptors in the macula were obtained as previously described.[14,20] Cone spacing measures were performed by two independent observers (KET and AR) who were masked to the treatment assignment of each eye during analysis. Severe cystoid macular edema and vitreous opacities precluded acquisition of AOSLO images in the sham-treated eye of patient 3 (Fig. 1C). Because media opacities, weakly reflecting cones, and blood vessels precluded visualization of a contiguous cone mosaic across the AOSLO image at every visit, we adopted three different methods to quantify the change in cones over time: cone spacing, cone density and cone tracking. All analyses involved selecting regions of interest (ROIs) in which unambiguous mosaics of cones were seen.

Cone spacing analyses are least affected by image quality variations because this method does not require identification of every cone within the ROI. If enough nearest neighbors are identified, a histogram of all intercone distances within the set will reveal the average nearest neighbor distance.[14,20,22] For cone spacing, ROIs were selected in which unambiguous cones were visualized at each of the two baseline visits by two investigators who were masked to treatment assignment. ROIs selected for cone spacing analyses were 0.56° to 1.96° from the fovea in the sham-treated eye and 0.87° to 2.42° in the CNTF-treated eye in patient 1, 0.53° to 3.08° from the fovea in the sham-treated eye and 0.85° to 2.19° in the CNTF-treated eye in patient 2, and 0.74° to 1.46° from the fovea in the CNTF-treated eye in patient 3. Average cone spacing at these prospectively determined ROIs was computed at 3, 6, 12, 18, 24, and 30 months after surgery and compared with similar locations in three age-similar normal subjects followed over 13 to 53 months.

Cone density analysis creates stricter demands on image quality because it requires that all cones within an ROI be identified; therefore, the power of the cone density measurement is greater than cone spacing. The total number of cones whose centers fall within the ROI is divided by the area to compute the number of cones/degree^2. ROIs for cone density were prospectively selected where all cones could be identified in one of the baseline montages, and a second measurement was taken at least 12 months later. Cone density locations were 0.51° to 1.60° from the fovea in the sham-treated eye and 0.56° to 1.42° in the CNTF-treated eye in patient 1; locations ranged from 1.72° to 3.00° in the sham-treated eye and 1.31° to 2.32° in the CNTF-treated eye; in patient 3, cone density locations were 0.97° to 1.44° in the CNTF-treated eye. The error in cone density estimates was attributed to cone selection (3 of 50 misidentified cones, or ±6%), spectacle magnification errors (~1%), distortion in cone images from eye motion (~1%), and selection of ROI (~1%). Assuming the errors to be random and independent, a conservative estimate of the error in cone density is ±6.3%.

Finally, individual cone tracking is possible when the image quality is ideal and the cone mosaic has not changed. In an individual cone tracking analysis, a direct cone-to-cone match is a definitive measure of lack of progression.

Statistical Analysis

We conducted pooled linear regression for visual function and OCT thickness measures. Time after implant, experimental status, and patient were included as regressors. Linear mixed models were used to fit repeated-measures observations for cone spacing for each ROI over time. We used the log cone spacing as the outcome, and we used the following as fixed-effect regressors: distance from the fovea of each region, patient, time, eye status (experimental, diseased control, normal), and interaction between eye status and time. A random intercept was used for each region. The model was fit (SAS Proc Mixed, version 9; SAS Institute, Cary NC), with the Kenward-Roger[23] adjustment for degrees of freedom. The same method (and regressors) was used with cone density observations. Postexplant times were excluded. Bonferroni adjustment for multiple comparisons indicated values smaller than 0.005 could be considered statistically significant at the 0.05 level (adjusting for 10 analyses). We conducted a sensitivity analysis for the cone spacing data. We assumed a spatial autocorrelation between regions in the same eye (accounting for multiple observations per person) and a temporal autocorrelation between observations taken in the same region. This analysis yielded results essentially identical to those reported ($P < 0.0001$).

Results

Clinical Characteristics

Patient 1 (autosomal dominant retinitis pigmentosa [adRP] with a rhodopsin mutation) received a higher-dose implant that

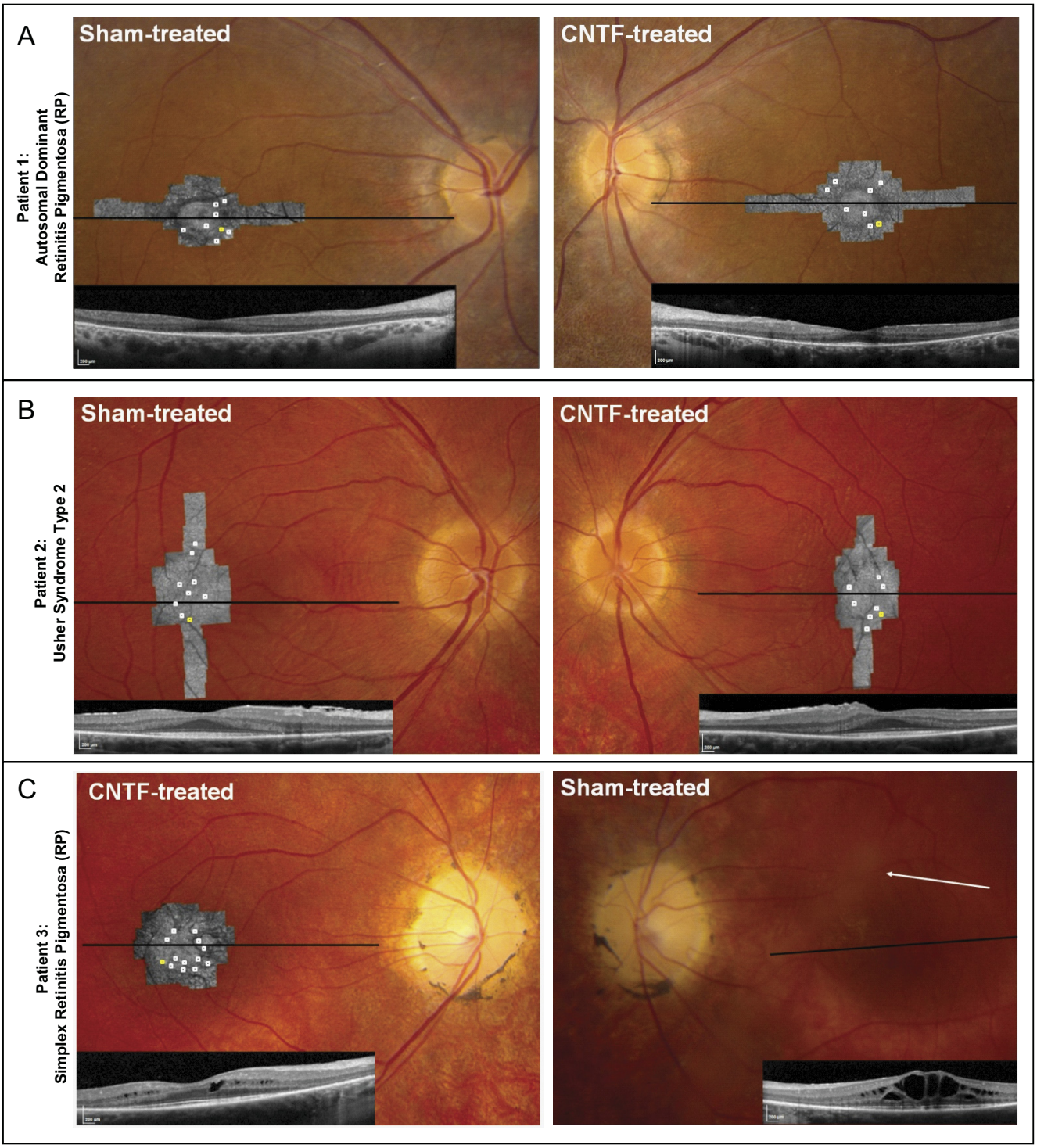

FIGURE 1. Retinal and AOSLO images. For each patient, fundus photographs are shown with AOSLO images and foveal horizontal spectral-domain optical coherence tomography (OCT) scans superimposed (*horizontal lines*: OCT scan location; *white squares* on AOSLO images: ROIs where cone spacing was analyzed in each AOSLO image over 30 months; *yellow squares*: retinal locations of density examples shown in Fig. 2). (**A**) Sham-treated and CNTF-treated eyes of patient 1. (**B**) Sham-treated and CNTF-treated eyes of patient 2. Bilateral epiretinal membranes on OCT images. (**C**) CNTF-treated and sham-treated eyes of patient 3. No AOSLO images were acquired in the sham-treated eye of patient 3 because of severe cystoid macular edema and vitreous opacities (*arrow* points to opacity obscuring retinal detail).

was secreting 1.42 ng CNTF/d when the patient elected to have it removed after 30 months because she wanted to become pregnant and the effects of maternal intraocular CNTF exposure on fetal development, if any, are unknown. Patients 2 (Usher syndrome type 2) and 3 (simplex RP) received lower-dose CNTF implants. Patient 3's implant was secreting 0.45 ng CNTF/d when she elected to have it removed after 24 months because she, too, wanted to become pregnant. Patient 2 elected to retain the implant at the end of the study. No ocular or systemic adverse events as defined by the study protocol were observed in any of the three patients during the study period (Table 1).

Table 1. Clinical Characteristics of Patients before and 24 Months after Implantation of Sustained-Release CNTF Delivered by Encapsulated Cell Technology

Patient	Age (y)/ Sex	Disease/ Mutation	Eye	BCVA before*/ 24 mo	ETDRS Score before*/ 24 mo	Foveal Threshold (dB) before†/ 24 mo	Total Visual Field Sensitivity (dB)‡ before/24 mo	Rod ERG b-Wave Amplitude§ (μV) before/24 mo	Rod ERG b-Wav e Timing (ms)§ before/24 mo	Cone ERG Flicker Amplitude§ (μV) before/24 mo	Cone Flicker Timing (ms)§ before/24 mo	TD-OCT Central Foveal Thickness (μm)‖ before/24 mo	SD-OCT Central Foveal Thickness (μm)¶ 12 mo/24 mo
1	33/F	ADRP/ heterozygous rhodopsin mutation (Gly51Val)	Right (sham treated)	20/25; 20/16	83/89	38.5/38.5	685/723	39/38	86/102.5	50/32	32/34.5	168/164	221/220
			Left (CNTF treated)	20/20; 20/20	86/85	38.5/38.0	691/619	37/29	86.5/103.5	50/43	31/30.5	168/210	245/256
2	29/M	Usher's syndrome type II simplex/ unknown	Right (sham treated)	20/20; 20/20	86/85	36/39.2	1504/1485	ND/ND	ND/ND	3/3	40/46.5	239/235	305/304
			Left (CNTF treated)	20/20; 20/20	86/88	37.1/38.5	1395/1418	ND/ND	ND/ND	3/3	41/45.5	239/235	319/314
3	27/F	RP simplex/ unknown	Right (CNTF treated)	20/20; 20/20	85/85	38.5/40.2	644/828	ND/ND	ND/ND	5.0/1.8	34/31	226/195	301/307
			Left (sham treated)	20/25; 20/32	79/74	38.8/37.0	667/860	ND/ND	ND/ND	2.5/2.6	31/31.5	235/255	423/417
				$P = 0.09$	$P = 0.15$	$P = 0.63$	$P = 0.07$			$P = 0.28$	$P = 0.95$	$P = 0.005$	$P < 0.001$

Before indicates baseline or most recent visit within 12 months before first baseline visit. *P* values represent results of pooled regression analyses as described. Regression analysis was not performed on rod- mediated ERG data because responses were not detectable in 2 of 3 patients. Patient 3 was excluded from analysis of foveal thickness. ND, not detectable.

* BCVA and ETDRS before values are best measures taken over three visits at baseline.

† Foveal threshold before value is average of six measures taken over three visits at baseline.

‡ Total visual field sensitivity represents the sum of visual field values from all four quadrants; before value is average of six measures taken over three visits at baseline.

§ Expressed as a percentage of the normal mean amplitude (rod, 272 μV; cone flicker, 121 μV), 2 SD below normal is 65% for rod b-wave and 54% for cone flicker, normal rod timing is <105 ms, and normal cone flicker timing is <32 ms.

‖ Time domain OCT central foveal thickness normal = 202.3 ± 19.6 μm (SD).

¶ Spectral-domain OCT central foveal thickness normal = 271.4 ± 19.6 μm (SD).[21]

Visual Function Measures

There was no significant difference in visual acuity, ETDRS score, foveal sensitivity, visual field sensitivity, photopic single flash, or flicker ERG amplitude or timing over 30 months between CNTF-treated and sham-treated eyes (Table 1). There was no significant change in any of these measures from baseline in either CNTF-treated or sham-treated eyes over 30 months.

Structural Measures

At baseline, foveal thickness in patient 1 was symmetric in each eye (Fig. 1A). In patient 2, foveal thickness was symmetric and slightly increased with bilateral epiretinal membranes (Fig. 1B). Patient 3 had cystoid macular edema in each eye at baseline that was more severe in the sham-treated eye and that fluctuated during the study (Fig. 1C). Because the cystoid macular edema restricted our ability to identify a CNTF-related effect on retinal thickness, OCT data from patient 3 were excluded from analysis.

Time-domain OCT showed central foveal thickness was 16.5 (95% confidence interval [CI], 7.2–25.7) μm greater (P = 0.005) and foveal macular volume was 0.43 (95% CI, 0.15–0.70) mm^3 larger in CNTF-treated than in the sham-treated eyes (P = 0.009). Spectral-domain OCT showed central foveal thick-

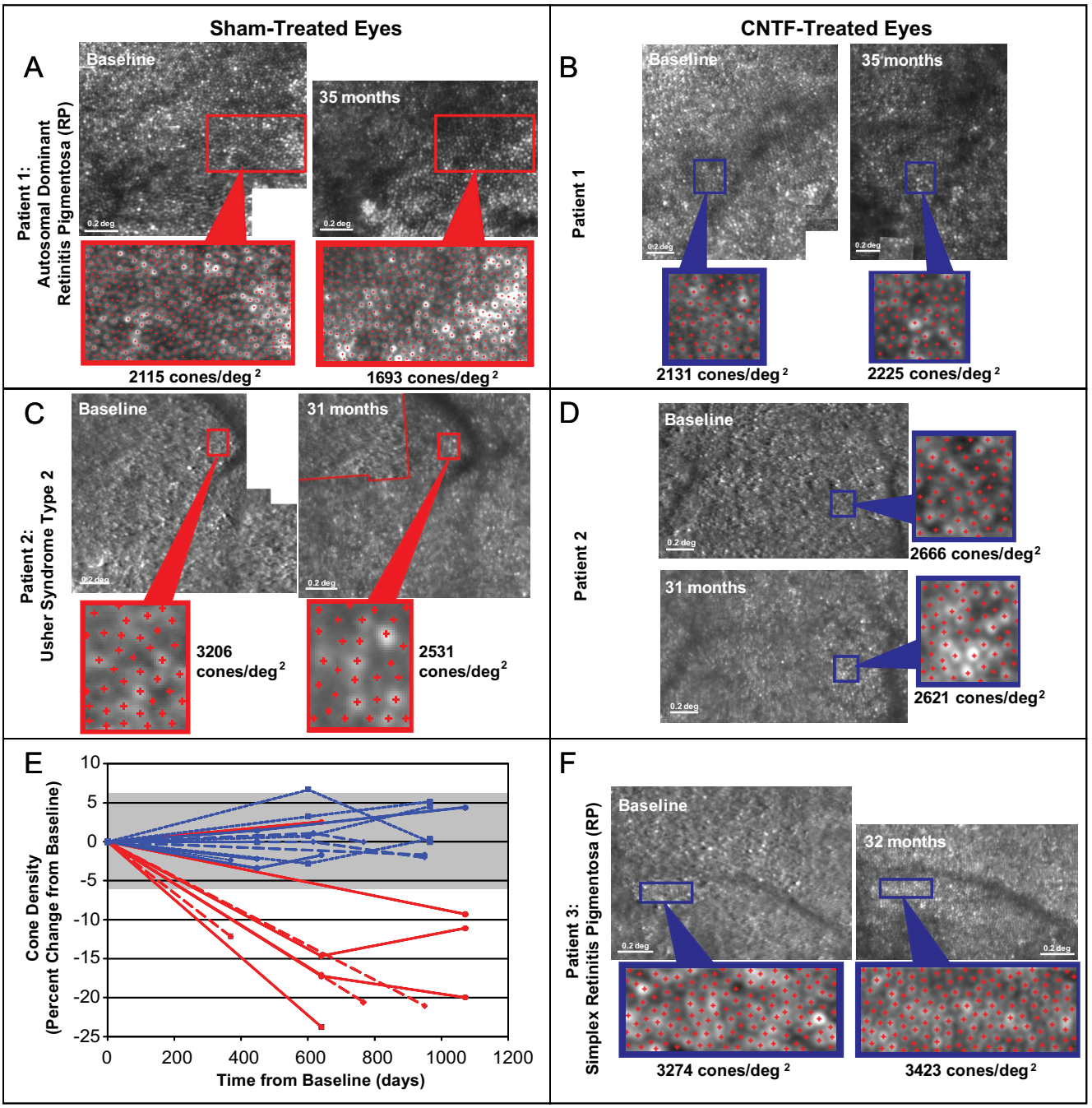

Figure 2. Cone photoreceptor density using AOSLO. Examples of paired AOSLO images at baseline and post-treatment in patient 1 sham (**A**) and CNTF-treated (**B**), patient 2 sham (**C**) and CNTF-treated (**D**), and patient 3 CNTF-treated (**F**) eyes in which cone density measurements were made (*yellow squares*, Fig. 1). *Red dots*: cones identified for density analysis. (**E**) Cone density over time in sham (*red*, n = 9) and CNTF-treated (*blue*) eyes (n = 12). *Solid lines*: patient 1; *long dashed line*: patient 2; *short dashed lines*: patient 3; *gray bar*: measurement error (±6.3%).

ness was 22.8 (95% CI, 16.8–28.9) μm greater ($P < 0.001$) and foveal volume was 0.21 (95% CI, 0.15–0.27) mm^3 larger ($P < 0.001$) in CNTF-treated eyes than in sham-treated eyes. Both time-domain and spectral-domain OCT images demonstrated increased thickness of the outer retinal layers, in which photoreceptor nuclei and inner and outer segments reside, in CNTF-treated eyes.

Cone Photoreceptor Structure Analysis from AOSLO Images

Three methods were used to quantify the changes in cone photoreceptors: cone spacing, cone density, and cone tracking.

Cone Spacing

ROIs were selected for cone spacing analyses longitudinally at similar eccentricities in each eye imaged (Fig. 1, white boxes). Severe cystoid macular edema and vitreous opacities precluded acquisition of AOSLO images in the sham-treated eye of patient 3 (Fig. 1C). Cone spacing increased significantly over time in 8 of 15 (53%) ROIs in sham-treated eyes but did not increase significantly in any ROIs (0/26) in the CNTF-treated eyes. Taken together, cone spacing increased by 2.9% (95% CI, 1.8%–4.1%) or by 0.042 arcmin (95% CI, 0.026–0.059) more per year in the sham-treated eyes than in CNTF-treated eyes ($P < 0.001$, linear mixed model). Repeated-measures analysis of cone spacing included three normal eyes that showed no increase in cone spacing in 13 ROIs followed for 16 to 53 months. There was no significant difference in the rate of cone spacing change between CNTF-treated eyes and normal eyes ($P = 0.20$).

Cone Density

Cone density was measured within selected ROIs at baseline and at least one subsequent imaging session 12 to 35 months later (Figs. 1, 2). Cone density decreased by 9% to 24% in 5 of 6 (83%) locations in the sham-treated eye but remained stable in 4 of 4 locations (100%) in the CNTF-treated eye of patient 1. Cone density decreased by 12% to 21% in 3 of 3 locations (100%) in the sham-treated eye but remained stable in 4 of 4 locations (100%) in the CNTF-treated eye of patient 2. Cone density remained stable in 4 of 4 (100%) locations in the CNTF-treated eye of patient 3. Overall, cone density decreased by 9% to 24% in 8 of 9 locations (89%) in sham-treated eyes but remained stable in 12 of 12 (100%) locations in the CNTF-treated eyes, changing less than the range of estimated measurement error (±6.3%; Fig. 2E). Within the selected regions, cone density decreased by 9.1% (95% CI, 6.6%–11.6%) or 223 (95% CI, 158–288) cones/degree^2 more per year in sham-treated than in CNTF-treated eyes ($P = 0.002$, linear mixed model).

Individual Cone Tracking

When images are of ideal quality, individual cones can be identified within a mosaic and monitored longitudinally. In a normal eye, virtually all cones were seen, and only 8 of 1906 cones (0.4%) were not visualized when the same location was imaged 53 months later (Fig. 3A). In the CNTF-treated eye of patient 3, individual cones were followed without significant change over 32 months, indicating that no measureable progression occurred at this location (Fig. 3B).

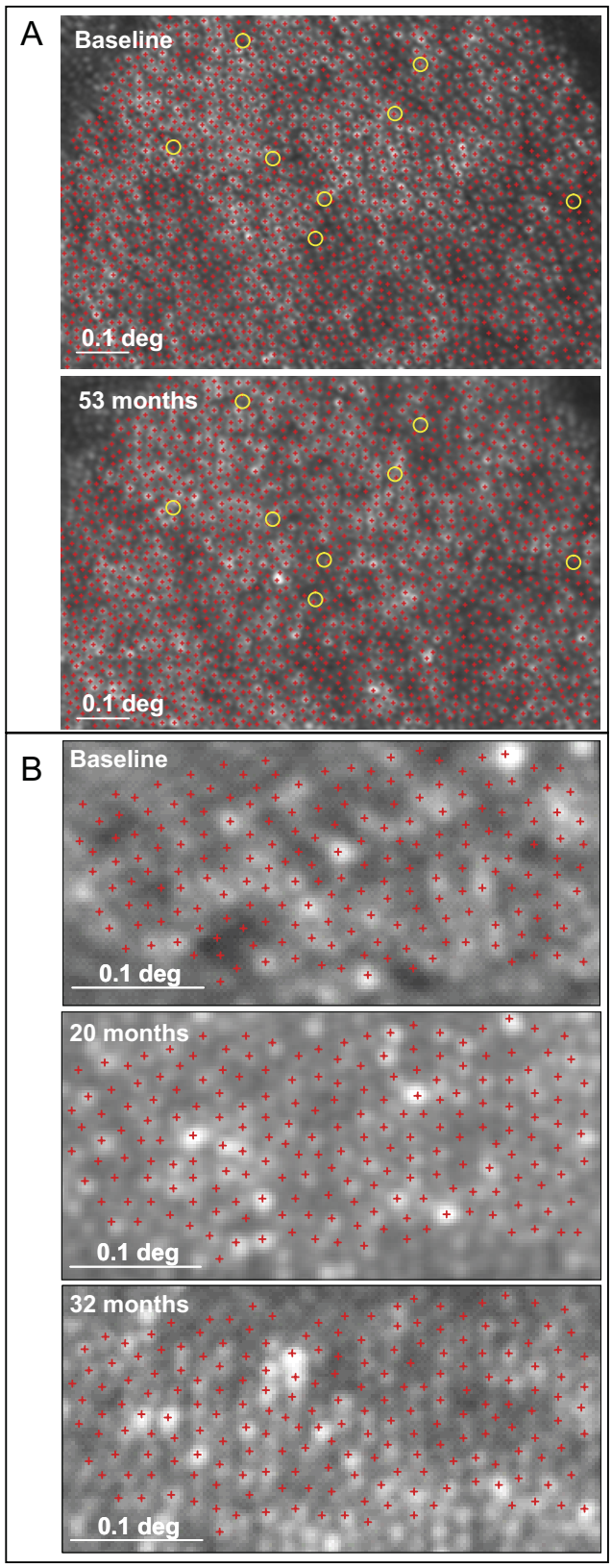

Figure 3. Cone photoreceptor tracking using AOSLO. (**A**) Individual cones (*red crosses*) are visible within a mosaic in a normal subject at baseline (*top*) and 53 months later (*bottom*). *Yellow circles*: cones (8/1906 or 0.4%) that were not seen 53 months later. (**B**) Individual cones are visible within a mosaic in the CNTF-treated eye of patient 3 at baseline (*top*), 20 months (*middle*), and 32 months (*bottom*) and show no loss over 32 months.

Discussion

This study presents the first images of cone photoreceptors in normal eyes monitored longitudinally and in patients with

retinal degeneration during disease progression and in response to CNTF therapy. Previous studies have used AOSLO to describe cone spacing and density in normal and diseased eyes, but have not reported changes in cone structure during retinal degeneration or in response to treatment.[11,13–20]

In the present study, we observed significant cone loss in the sham-treated eyes of patients 1 and 2 at most retinal locations over the 35-month study period. In contrast, in all three patients, AOSLO images showed significantly reduced rates of cone loss in CNTF-treated eyes compared with contralateral sham-treated eyes. Cone spacing changes in CNTF-treated eyes were not significantly different from those in normal eyes studied over similar periods. No significant decrease in cone density was observed in the CNTF-treated eyes. In some locations with ideal image quality, individual cones were followed within a mosaic over 32 months in an eye with retinal degeneration that received CNTF. Taken together, these data suggest that exposure to sustained-release CNTF was associated with reduced cone loss.

Foveal thickness was significantly increased in CNTF-treated eyes. CNTF treatment causes increased euchromatin and outer nuclear layer thickness in animal models of retinal degeneration.[24–27] We observed increased retinal thickness at the fovea in eyes with inherited retinal degenerations treated with CNTF. At the fovea, the retinal thickness consists of the outer nuclear layer and the inner and outer segment layers, where the photoreceptors are located. The increased thickness measured with OCT in eyes treated with CNTF may be consistent with the increased thickness of the outer nuclear layer and photoreceptor inner and outer segment layers observed in histologic studies of animal models of retinal degeneration treated with CNTF.[24–27] Taken together with the en face images acquired using AOSLO, the present study demonstrates reduced cone loss in eyes treated with CNTF, which should ultimately result in improved outcomes for patients with retinal degeneration.

Patients in the present study showed no significant changes in visual acuity, visual field, or ERG responses. Several factors complicate analyses of visual function as an outcome measure for clinical trials in patients with retinal degeneration. Retinal degeneration tends to progress slowly over years, so severe photoreceptor loss must occur before reliable, significant differences are measureable in visual function.[7–9] ERG measures global outer retinal function and is often reduced below measurable levels in this patient population, whereas visual acuity is often preserved despite advanced retinal degeneration. Although no significant changes in any standard clinical measures of retinal degeneration were observed during the study period, we observed significant changes in cone spacing and density in sham-treated eyes of a patient with adRP and a patient with Usher syndrome type 2. Our results suggest that direct observation and analysis of high-resolution images of cone structure may provide a sensitive, objective measure of disease progression and treatment response in patients with inherited retinal degenerations over a 2-year period.

The study is limited by the small number of eyes evaluated and the number of retinal locations analyzed. Intraretinal variation in cone spacing and density was observed, and it is possible that the areas analyzed were not representative of the entire retina. Our analyses are based on regions in which cones were visualized unambiguously and likely represent a conservative estimate of the severity of retinal degeneration. However, similar locations were analyzed in both CNTF- and sham-treated contralateral eyes to minimize the likelihood that selection bias produced the differences observed. Cone spacing measures were performed by two investigators who were masked to the treatment assignment. However, the more sensitive measures of cone density and cone tracking were developed after the cone spacing data had been analyzed, and the investigators were not masked to treatment assignment when they identified regions in which every cone was visualized. The differences in rates of change of cone spacing and cone density between sham- and CNTF-treated eyes are larger than would be expected because of image analysis artifact or bias. However, as future clinical trials of CNTF are initiated, the methods designed to quantify cone spacing, density, and tracking measures for this study should be used in a prospective, fully masked fashion, such that the results from a larger study will more conclusively support or refute the hypothesis that CNTF is effective in slowing the rate of photoreceptor loss in patients with inherited retinal degenerations.

We were unable to evaluate visual function of the cones that were imaged on an individual cellular level. AOSLO can be used to deliver stimuli to individual cones and measure visual function with high resolution,[18,28] but this technique is not yet fully developed to study eyes with inherited retinal degeneration. Future studies, however, could use AOSLO to evaluate retinal function in regions in which cones are visualized longitudinally in patients with retinal degeneration.

The results suggest that AOSLO can provide a sensitive measure of disease progression and treatment response in patients with retinal degeneration. In this study presenting the first images of cone photoreceptors in human eyes treated with CNTF, the results suggest that CNTF may slow cone photoreceptor loss in eyes with retinal degeneration. They also provide evidence to support the pursuit of additional, larger, prospective, masked clinical trials of CNTF using AOSLO images as an outcome measure of disease progression and treatment response. Further studies are urgently needed of cone structure during retinal degeneration and in response to CNTF treatment. Additional studies should evaluate larger numbers of patients longitudinally with high-resolution measures of cone structure using AOSLO.

Acknowledgments

The authors thank Matthew M. LaVail, Eugene de Juan, Jr, and John Dowling for their input on drafts of the manuscript, Arshia Mian for clinical trial coordination, and Pavan Tiruveedhula for computer software engineering to facilitate AOSLO image acquisition.

References

1. Hartong DT, Berson EL, Dryja TP. Retinitis pigmentosa. *Lancet.* 2006;368:1795–1809.
2. Fishman GA. Challenges associated with clinical trials for inherited and orphan retinal diseases. *Retina.* 2005;25:S10–S12.
3. LaVail MM, Unoki K, Yasumura D, Matthes MT, Yancopoulos GD, Steinberg RH. Multiple growth factors, cytokines, and neurotrophins rescue photoreceptors from the damaging effects of constant light. *Proc Natl Acad Sci U S A.* 1992;89:11249–11253.
4. MacDonald IM, Sauve Y, Sieving PA. Preventing blindness in retinal disease: ciliary neurotrophic factor intraocular implants. *Can J Ophthalmol.* 2007;42:399–402.
5. Li Y, Tao W, Luo L, et al. CNTF induces regeneration of cone outer segments in a rat model of retinal degeneration. *PLoS One.* 2010; 5:e9495.
6. Sieving PA, Caruso RC, Tao W, et al. Ciliary neurotrophic factor (CNTF) for human retinal degeneration: phase I trial of CNTF delivered by encapsulated cell intraocular implants. *Proc Natl Acad Sci U S A.* 2006;103:3896–3901.
7. Fishman GA, Bozbeyoglu S, Massof RW, Kimberling W. Natural course of visual field loss in patients with type 2 Usher syndrome. *Retina.* 2007;27:601–608.
8. Grover S, Fishman GA, Anderson RJ, Alexander KR, Derlacki DJ. Rate of visual field loss in retinitis pigmentosa. *Ophthalmology.* 1997;104:460–465.
9. Iannaccone A, Kritchevsky SB, Ciccarelli ML, et al. Kinetics of visual field loss in Usher syndrome type II. *Invest Ophthalmol Vis Sci.* 2004;45:784–792.

10. Liang J, Williams DR, Miller DT. Supernormal vision and high-resolution retinal imaging through adaptive optics. *J Opt Soc Am A Opt Image Sci Vis.* 1997;14:2884–2892.
11. Roorda A, Romero-Borja F, Donnelly W III, Queener H, Hebert T, Campbell M. Adaptive optics scanning laser ophthalmoscopy. *Opt Express.* 2002;10:405–412.
12. Zhang Y, Poonja S, Roorda A. MEMS-based adaptive optics scanning laser ophthalmoscopy. *Opt Lett.* 2006;31:1268–1270.
13. Choi SS, Doble N, Hardy JL, et al. In vivo imaging of the photoreceptor mosaic in retinal dystrophies and correlations with visual function. *Invest Ophthalmol Vis Sci.* 2006;47:2080–2092.
14. Duncan JL, Zhang Y, Gandhi J, et al. High-resolution imaging with adaptive optics in patients with inherited retinal degeneration. *Invest Ophthalmol Vis Sci.* 2007;48:3283–3291.
15. Li KY, Roorda A. Automated identification of cone photoreceptors in adaptive optics retinal images. *J Opt Soc Am A Opt Image Sci Vis.* 2007;24:1358–1363.
16. Rha J, Dubis AM, Wagner-Schuman M, et al. Spectral domain optical coherence tomography and adaptive optics: imaging photoreceptor layer morphology to interpret preclinical phenotypes. *Adv Exp Med Biol.* 2010;664:309–316.
17. Roorda A, Zhang Y, Duncan JL. High-resolution in vivo imaging of the RPE mosaic in eyes with retinal disease. *Invest Ophthalmol Vis Sci.* 2007;48:2297–2303.
18. Rossi EA, Roorda A. The relationship between visual resolution and cone spacing in the human fovea. *Nat Neurosci.* 2010;13:156–157.
19. Wolfing JI, Chung M, Carroll J, Roorda A, Williams DR. High-resolution retinal imaging of cone-rod dystrophy. *Ophthalmology.* 2006;113:1019 e1011.
20. Yoon MK, Roorda A, Zhang Y, et al. Adaptive optics scanning laser ophthalmoscopy images in a family with the mitochondrial DNA T8993C mutation. *Invest Ophthalmol Vis Sci.* 2009;50:1838–1847.
21. Grover S, Murthy RK, Brar VS, Chalam KV. Comparison of retinal thickness in normal eyes using Stratus and Spectralis optical coherence tomography. *Invest Ophthalmol Vis Sci.* 2010;51:2644–2647.
22. Rodieck RW. The density recovery profile: a method for the analysis of points in the plane applicable to retinal studies. *Vis Neurosci.* 1991;6:95–111.
23. Kenward MG, Roger JH. Small sample inference for fixed effects from restricted maximum likelihood. *Biometrics.* 1997;53:983–997.
24. Liang FQ, Aleman TS, Dejneka NS, et al. Long-term protection of retinal structure but not function using RAAV.CNTF in animal models of retinitis pigmentosa. *Mol Ther.* 2001;4:461–472.
25. Bok D, Yasumura D, Matthes MT, et al. Effects of adeno-associated virus-vectored ciliary neurotrophic factor on retinal structure and function in mice with a P216L rds/peripherin mutation. *Exp Eye Res.* 2002;74:719–735.
26. Wen R, Song Y, Kjellstrom S, et al. Regulation of rod phototransduction machinery by ciliary neurotrophic factor. *J Neurosci.* 2006;26:13523–13530.
27. Rhee KD, Ruiz A, Duncan JL, et al. Molecular and cellular alterations induced by sustained expression of ciliary neurotrophic factor in a mouse model of retinitis pigmentosa. *Invest Ophthalmol Vis Sci.* 2007;48:1389–1400.
28. Sincich LC, Zhang Y, Tiruveedhula P, Horton JC, Roorda A. Resolving single cone inputs to visual receptive fields. *Nat Neurosci.* 2009;12:967–969.